Werk

Jahr: 1985
Kollektion: fid.geo
Signatur: 8 Z NAT 2148:57
Digitalisiert: Niedersächsische Staats- und Universitätsbibliothek Göttingen
Werk Id: PPN1015067948_0057
PURL: http://resolver.sub.uni-goettingen.de/purl?PPN1015067948_0057

LOG Id: LOG_0032
LOG Titel: In-situ permeability from non-dilatational soil deformation caused by groundwater pumping - a case study
LOG Typ: article

Übergeordnetes Werk

Werk Id: PPN1015067948
PURL: http://resolver.sub.uni-goettingen.de/purl?PPN1015067948
OPAC: http://opac.sub.uni-goettingen.de/DB=1/PPN?PPN=1015067948

Contact

Niedersächsische Staats- und Universitätsbibliothek Göttingen
Georg-August-Universität Göttingen
Platz der Göttinger Sieben 1
37073 Göttingen
Germany
Email: gdz@sub.uni-goettingen.de

J Geophys (1985) 57:184–190

Journal of Geophysics

In-situ permeability from non-dilatational soil deformation caused by groundwater pumping – a case study

H.-J. Kümpel [1], **G. Lohr** [2]

[1] Dalhousie University, Halifax, Canada; now at University of Kiel, Federal Republic of Germany
[2] University of Kiel, Federal Republic of Germany

Abstract. Short-term disturbances in the recording of a sensitive borehole tiltmeter are found to be generated by groundwater pumping at 120 m distance. Biot's consolidation theory for elastic porous media is applied to simulate the physical process involved. Results from various finite-element calculations for axisymmetric conditions are obtained. The findings are:

(1) The observed tilt disturbances can be explained as being provoked by elastic consolidation phenomena.

(2) Non-dilatational tilt and strain deformations can be measured outside the region where the pore pressure has declined due to pumping.

(3) The time variation of the deformations constrains the in-situ permeability of the aquifer within some volume around the screen of the pumped well.

The fundamentals of this case study may be useful to hydrologists and to those investigators who set up high-resolution tilt and/or strain measurements for purposes of geodynamic interest.

Key words: In-situ permeability – Soil deformation – Pump tests – Aquifer parameters – Tilt and strain measurements

Introduction

Methods to estimate aquifer parameters from pressure variations in a well have been described by different authors. Some of them investigated well tides from aquifer dilatation caused by earth tides or ocean loading tides (Bredehoeft, 1967; Robinson and Bell, 1971; Rhoads and Robinson, 1979), or considered well level undulations due to tidal gravity changes on the aquifer's overburden (Morland and Donaldson, 1984). Others analysed well pressure fluctuations due to volumetric strains caused by seismic disturbances (Cooper et al., 1965). These pressure variations are reported to be significant only if measured in confined aquifers. Soil parameters from artificially forced well level oscillations have been obtained by Krauss (1974). Unlike the methods relying on natural forcing functions, the latter technique is equally applicable to unconfined aquifers.

In many cases, satisfactory estimates can be made for pore fluid viscosities, temperatures, densities, compressibilities and shear moduli of formations. The quantities derived from well pressure variations are therefore used to estimate the in-situ porosity and permeability of the aquifer. Under favourable conditions, the penetration depth related to the various methods extends from some ten to hundred metres, depending on the periods of the pressure variations and on the transmissivity of the aquifer (Bodvarsson, 1970; Krauss, 1974; Varga, 1976).

We present a case study showing how in-situ permeability of an unconfined aquifer is estimated from soil deformations caused by pumping. Since the deformations are sensed by a tiltmeter which is installed in a borehole situated away from the pumped well, mainly the non-dilatational part of the total deformation field is observed. The volume of the aquifer derived by this technique is probably larger than for the methods mentioned above.

The physical process involved is described by Biot's widely used consolidation theory (Biot, 1941). A load, when applied to a porous elastic medium, yields instantaneous deformation by compression of both the porous skeleton, called the matrix, and the pore filling. Further deformation of the medium arises from body forces; namely, from internal pore pressure gradients that are stimulated by the compression. These forces vary with time since the pressure gradients decrease through diffusion until a new steady-state equilibrium is achieved. The time variation of the process is mainly governed by the permeability of the medium and the viscosity of the pore filling. Zschau (1979) applied Biot's theory to show that meteorological air pressure variations can account for systematic tilt anomalies that he observed several tens of metres below the slope of a hill.

In our case, the deformation of the aquifer results from the pore pressure gradient that is stimulated at the screen of the pumped well. The tilt amplitudes measured are 5–10 times smaller than the earth tidal tilt amplitude. This might be the reason why soil engineers and hydrologists have not, so far, considered the method as a possible tool to determine aquifer parameters, although the use of high-precision instruments will not always be an inevitable necessity. The findings also have implications for the implementation and interpretation of tilt and strain measurements in projects of geodynamic interest.

Observations

The Institute of Geophysics, Kiel, runs a tiltmeter station in the northern Federal Republic of Germany, close to the village of Medelby (Fig. 1). Former purposes of the site, built up in 1977, have been loading investigations in the

Offprint requests to: H.-J. Kümpel

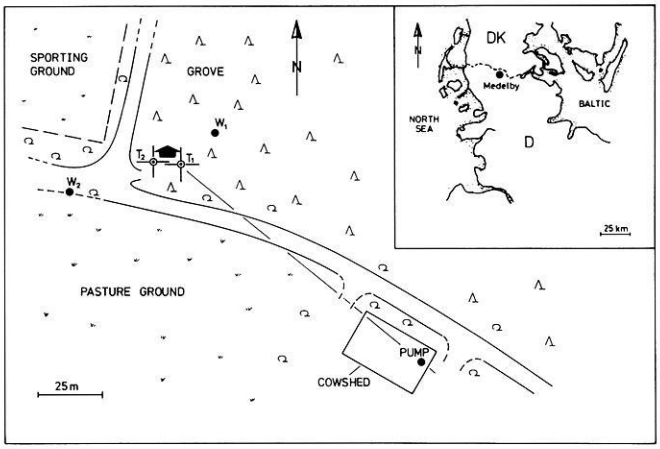

Fig. 1. Location map of the village of Medelby (DK = Denmark, D = Federal Republic of Germany) and of the tiltmeter site to the west of Medelby (T_1, T_2 = tiltmeter boreholes with registration hut; W_1, W_2 = groundwater observation wells)

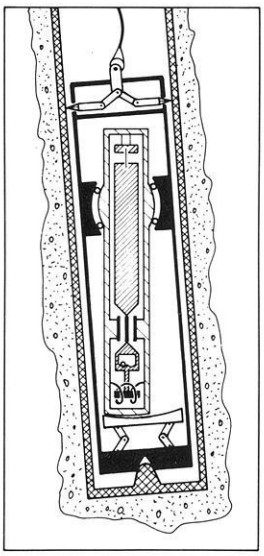

Fig. 2. Schematic cross-section of the major componenets of an Askania borehole tiltmeter with sensor pendulum (*heavy hatching*), pendulum holder (*light hatching*) and instrument casing (*black*). Elements of the sensor pendulum, from top to bottom, are: suspension strips, capacitance transducer, calibration chamber, and feedback magnet (inside coil). The lower end of the borehole ends in a cemented-in steel casing (*cross hatching*) that holds the instrument. When in operation, only the sensor pendulum hangs vertically

environments of the North Sea and the Baltic (Kümpel, 1982).

The tiltmeter we use is a continuously recording Askania-Gezeitenbohrlochpendel vertical pendulum type (Fig. 2). The top of the casing of the pendulum is clamped to the borehole by spring-loaded studs, its bottom resides on a stainless steel cone. Since the borehole is not vertical, the sensor pendulum hangs obliquely in the casing with respect to the instrument axis. To allow for a greater obliqueness of the borehole and for a wider measuring range without loss of sensitivity, the sensor pendulum is suspended in a pendulum holder which itself hangs in a nearly vertical position. Prior to operation of the tiltmeter, the pendulum holder is fixed to the casing by raising a

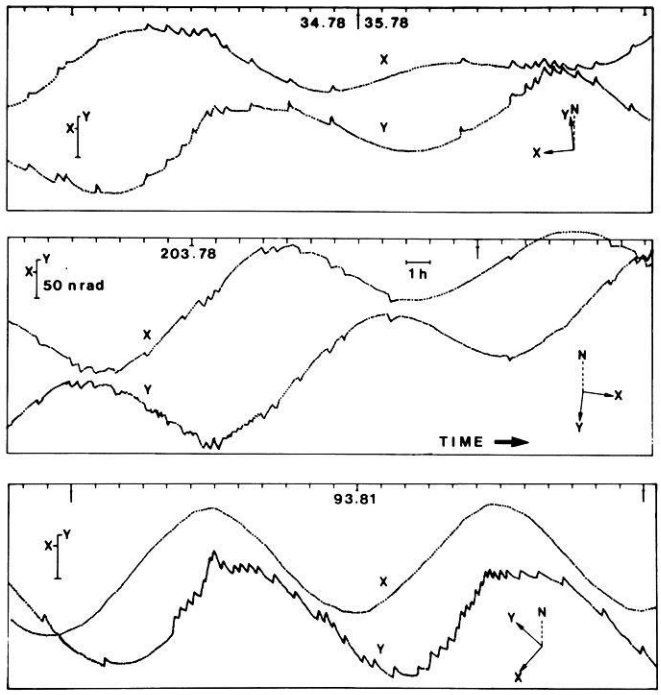

Fig. 3. Tilt disturbances 30 m below surface from pumping activities at 120 m distance. Graphs are tiltmeter recordings with components x and y at different azimuths (as indicated). The lower end of the tiltmeter borehole is always dragged towards the pump at 130° E of N; thus, on day number 93 in 1981 (*lower graph*), y is deflected towards 310°E of N with no disturbances in x. Long periodic undulations are tides

base plate. Tilt of the sensor pendulum with respect to the pendulum holder is sensed by a capacitance transducer. Calibration is achieved by forcing a steel ball to hop from one of two notches to the other within a small chamber. A feedback system made of coils and magnets provides active damping and raises the linear range of the instrument. The 60-cm-long sensor pendulum is suitable for measuring tilt in two perpendicular axes because of suspension strips that allow movements in any direction. Within the diurnal tidal bands, the instrumental resolution is 1 nrad ($\approx$0.2 mseca).

Due to microseismicity, the noise level at the site varies between 2 and 6 nrad. Besides the tidal signal and strong rainfall-induced tilt anomalies, we observe short-term tilt disturbances of 15–20 nrad amplitude (Fig. 3). Occurrence of these disturbances coincides with groundwater pumping for agricultural use at 120 m distance. The events become visible on the tilt recording within 30 s after activation of the pump, as was proven by monitoring the switch times of the pump. The time of response of the tiltmeter to pumping could even be shorter since the tilt signal is low pass-filtered with a cutoff period of 20 s. Without filter, a potentially immediate tilt response is masked by microseismicity.

A single event has a sawtooth-like shape with its recovery lasting longer than its stimulation. The sign of the disturbances is clearly independent of the azimuthal orientation of the tiltmeter. For seven different orientations (three are shown in Fig. 3), the maximum tilt effect occurs in a north-west direction. Moreover, the effect is independent of the individual tiltmeter borehole. The upper recording

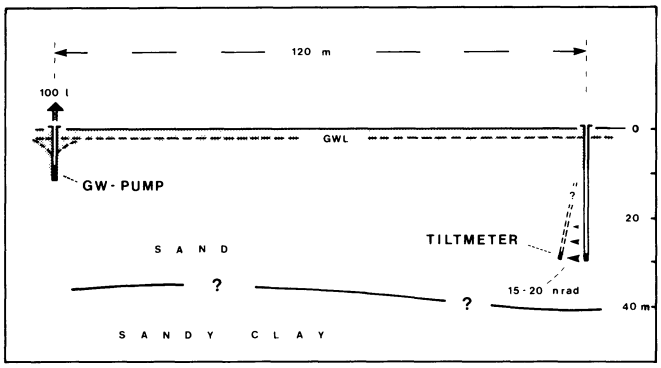

Fig. 4. Sketch of relevant features and proportions determining tilt disturbances at the Medelby site, northern FRG. Depth of intersection between sand and sandy clay layer is estimated from borehole information several hundred metres apart

in Fig. 3 is observed in hole T_1, the lower two are observed in hole T_2 (see Fig. 1). Both holes are 30 m deep; T_1 is PVC-cased, T_2 is iron-cased. As the top of the tiltmeter is clamped to the borehole at 28.5 m depth, the non-Newtonian part of the tilt signal indicates the change in inclination of a vertical element between 28.5 and 30 m depth.

Figure 4 is a section of the site along the line T_1 – pump in Fig. 1. The well and the tiltmeter boreholes (only one is shown) have been drilled into a sand layer. Depending on the season, the depth of the groundwater level varies between 1.5 and 3 m. The well extends 9 m into the aquifer. Only the lower 3 m are perforated to allow the water to enter through the well screen. The diameter of the well is about 20 cm (8 in.) including the filter, made of pebbles. The diameter of the tiltmeter borehole is also 8 in. The productivity of the pump is approximately 20 l/min. Some 100 l are pumped during a typical pumping cycle. Whenever the pump draws groundwater, the lower end of the tiltmeter borehole is dragged towards the pumped well located to the south-east of the tiltmeter, thereby generating a tilt signal that is strongest in the opposite azimuth. Theoretically, the tilt events might also result from deflections of the plumb-line towards the north-west with the tiltmeter borehole remaining in a fixed position. However, simple calculation shows that the Newtonian effect of lifting a 100-kg mass over a height of 5 m at 120 m distance deflects the vertical by some negligible 10^{-7} nrad only. Within 30 m distance of the tiltmeter boreholes, we operate two continuously running water-table gauges of 5 mm resolution each (W_1 and W_2 in Fig. 1). Neither of them monitors a lowering of the water-table due to the pumping.

From other holes drilled in the vicinity of the site, it is known that (a) the sand is partially intersected by thin clay and clay shale layers and (b) somewhere below 30–40 m the sand changes its character to sandy clay. A detailed stratigraphy is not available. Several samples from the upper 2 m of the sand layer have been subjected to sieve analysis. The sand is well sorted, the median grain diameter is 0.2 mm, the clay fraction being less than 5%. Intrinsic permeability for a single sample from 1-m depth has been repeatedly measured in a laboratory flow experiment. The values obtained range from 5×10^{-8} to 22×10^{-8}cm^2, in agreement with Davis (1969) who reports permeabilities from 10×10^{-8} to 22×10^{-8}cm^2 for five sands of this size. Applying classical draw-down relations for wells in unconfined aquifers (e.g. Brown et al., 1972), we calculate in-situ permeabilities in the range 1.5×10^{-8}–6×10^{-8}cm^2 when taking into account that the well only partially penetrates the aquifer.

Formulation of model calculations

The relation between elastic deformation and pore pressure is described by the theory of consolidation for porous media (Biot, 1941). If axial symmetry holds, the governing system of differential equations is (Verruijt, 1969):

$$\mu\nabla^2 u-\mu\frac{u}{r^2}+(\lambda+\mu)\frac{\partial\varepsilon}{\partial r}-\alpha\frac{\partial\sigma}{\partial r}=0$$

$$\mu\nabla^2 w+(\lambda+\mu)\frac{\partial\varepsilon}{\partial z}-\alpha\frac{\partial\sigma}{\partial z}=0 \qquad (1)$$

$$\frac{\alpha}{\lambda+\mu}\frac{\partial}{\partial t}\left(\frac{\sigma_r+\sigma_z}{2}\right)+\left(1-\frac{\lambda}{\lambda+\mu}\right)\frac{\alpha}{r}\frac{\partial u}{\partial t}+\left(\frac{\alpha^2}{\lambda+\mu}+S\right)\frac{\partial\sigma}{\partial t}=\frac{k}{\eta}\nabla^2\sigma$$

where the variables u (=radial displacement), w (=vertical displacement), σ (=excess pore pressure, with respect to the hydrostatic pressure) are functions of the coordinates r (=radius), z (=height) and t (=time). All forces are in equilibrium for t being negative, r is zero for the centre of the pore pressure disturbance, z is negative below the surface where the depth is positive.

$\nabla^2=\frac{\partial^2}{\partial r^2}+\frac{1}{r}\frac{\partial}{\partial r}+\frac{\partial^2}{\partial z^2}$ is the Laplacian operator,

$\varepsilon=\frac{\partial u}{\partial r}+\frac{u}{r}+\frac{\partial w}{\partial z}$
is the volume strain (positive for compression),

$(\sigma_r+\sigma_z)/2$ is the average total stress.

Soil parameters are:

μ = shear modulus,

λ = Lamé constant,

$\alpha=1-c_g/c_m$ with c_g = grain compressibility and $c_m=(\lambda+2\mu/3)^{-1}$ = compressibility of the porous matrix (after Nur and Byerlee, 1971),

$S=\rho\cdot c_f+(1-\rho)c_m$, i.e. the hydraulic capacity where ρ is the volume porosity and c_f is the compressibility of the fluid filling the pore (after Bodvarsson, 1970),

k = intrinsic permeability,

η = dynamic viscosity of the pore fluid.

Following the notation of Davis and De Wiest (1966), $S_S=\delta\cdot g\cdot S$ is the specific storage of the formation where δ is the density of the pore fluid and g is the gravitational acceleration, and $K=k\cdot\delta\cdot g/\eta$ is the hydraulic conductivity. μ, λ, c_m are bulk formations constants for quasi-static, i.e. drained conditions as compared to undrained conditions that hold for elastic wave propagation.

Equation (1) is based on infinitesimal strains, elastic deformation (i.e. linear reversible stress-strain relations), soil that is saturated with pore fluid, the validity of Darcy's law (i.e. no turbulent flow) and the absence of inertia forces. The first two equations result from introducing Hooke's generalized law for elastic porous media into the well-known equilibrium conditions. Considerations on fluid flow according to Darcy's law and on the elastic storage capacity

of prous media under pressure lead to the third equation. Because the change in pore pressure σ is relevant for each part of Eq. (1), the system has to be solved simultaneously. Since the third equation is not exactly analogous to any heat conduction problem that has been analysed, analytical solutions are rare and become complex, even for simple geometric configurations.

Numerous consolidation problems have instead been solved using the finite-element technique. The program package available to us (IMSL, 1983) allows a straightforward conversion of the problem into programming code when not more than one time-derivative term per equation is encountered. Two modifications of Eq. (1) are introduced to meet this condition. The first modification neglects any time variation in the average total stress term. The effect of this simplification on various geometrical configurations has been analysed by Christian and Boehmer (1970). They did not find severe divergences with respect to the complete models if external loads remain constant with time, which also holds in our case. Yet, our numerical solutions are applicable only if other geometric and parametric simplifications within the model are as coarse approximations to reality as the assumption of constant average total stress is.

The second modification substitutes σ by a new variable

$$\Phi = A \cdot u/r + B \cdot \sigma,$$

which alters Eq. (1) into:

$$\begin{aligned}
&\mu \nabla^2 u - \mu \frac{u}{r^2} + (\lambda+\mu)\frac{\partial \varepsilon}{\partial r} - \frac{\alpha}{B}\left[\frac{\partial \Phi}{\partial r} + \frac{A}{r}\left(\frac{u}{r} - \frac{\partial u}{\partial r}\right)\right] = 0 \\
&\mu \nabla^2 w \qquad + (\lambda+\mu)\frac{\partial \varepsilon}{\partial z} - \frac{\alpha}{B}\left(\frac{\partial \Phi}{\partial z} - \frac{A}{r}\frac{\partial u}{\partial z}\right) = 0 \qquad (2) \\
&\nabla^2 \Phi - \frac{A}{r}\left(\nabla^2 u - \frac{2}{r}\frac{\partial u}{\partial r} + \frac{u}{r^2}\right) = \frac{B\eta}{k}\frac{\partial \Phi}{\partial t}
\end{aligned}$$

$$\text{with } A = \left(1 - \frac{\lambda}{\lambda+\mu}\right)\alpha \quad \text{and} \quad B = \frac{\alpha^2}{\lambda+\mu} + S.$$

Tilt ψ of a vertical element at radius r, depth $z = (z_1 + z_2)/2$, and time t is obtained from

$$\tan^{-1} \psi\,(r, z, t) = \frac{u(r,z_2,t) - u(r,z_1,t)}{z_1 - z_2} \qquad (3)$$

if $|z_2 - z_1|$ is taken much larger than vertical displacements. By this convention, ψ is positive when the upper end of the element is closer to the axis than the lower end. Respective relations hold for strain of vertical elements and for tilt and strain of horizontal elements.

Figure 5 shows the spatial division of the model into 96 triangular elements. Along a line segment combining two nodes, quadratic fits are exerted on the variables. The thin, drained layer above the water-table is omitted which leads to somewhat reduced depths of the well and of the borehole. The load of the drawn groundwater that increases atop the pump during a pumping cycle before it is supplied to a system of pipes also is neglected. The saturated sand layer and the sandy clay layer are characterized by their parameters E, ν, ρ and k, where $E = 2\mu(1+\nu)$ is the Young's modulus of the formation and $\nu = 0.5\,\lambda\,(\lambda+\mu)^{-1}$ is its Poisson's ratio. The difference in grain compressibility c_g between the two layers is of minor importance only.

The upper part of the sandy clay layer is modelled by a sequence of thin elements. This has been found necessary

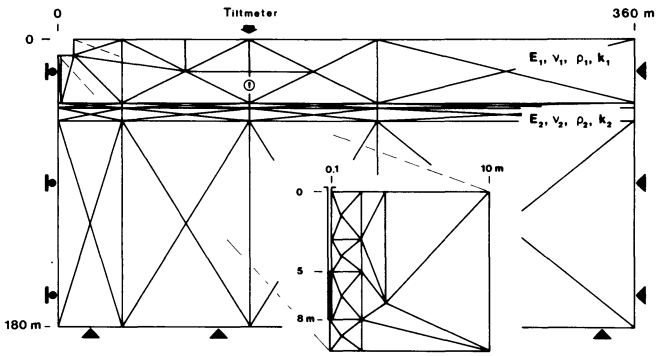

Fig. 5. Finite-element grid for modelling tilt disturbances in two-layered r-, z-plane (axial symmetry). The pump is located close to the *upper left corner* (see *enlarged section*). A pore pressure deficit is stimulated between 5 and 8 m depth on the *left boundary*

to simulate the pore pressure diffusion across a layer intersection with a permeability contrast as is assumed here. The accuracy of the model for the net diffusion process is better than 10% when compared to analytical solutions. A further grid refinement is arranged close to the pump where the highest gradients in the variables u, w, σ are encountered.

As for the boundary conditions; displacements and pore pressure variations are prohibited at the lower boundary surface and at the outer radius of the model ($r = 360$ m), only vertical displacements and pressure changes are tolerated for the zero-radius. We disregard changes in the size of the well caused by the pumping, nor do we consider the elastic properties of the tiltmeter borehole as being different from those in its vicinity. Initially, displacements and excess pore pressure are assumed to be zero everywhere. The pumping is induced by a step function: at $t = 0$ s, a constant pore pressure deficit of -200 hPa is applied at the well screen. Eq. (2) is then successively evaluated at times $t = 2^n$ s ($n = 1, 2, \ldots, 10$). Stability of the numerical results, in the sense of Booker and Small (1975), is achieved.

Computational results

Various models are tested. Parameters listed in Table 1 label the standard model. The static Young's moduli are deduced from a shallow seismic experiment at the site using theoretical and empirical relations between seismic velocities and static moduli for unconsolidated sediments (Ohkubo and Terasaki, 1977). In one of these relations, a Poisson's ratio of $\nu = 0.25$ is taken; we apply a more realistic value of $\nu = 0.45$ instead. The true static moduli might vary by up to $\pm 50\%$ of the values given in Table 1. Increasing E_1, E_2 by the same factor, mainly reduces the displacement amplitudes by the reciprocal factor. For k_1, the standard model adopts a value of $1.5 \times 10^{-8}\text{cm}^2$. Effects due to different permeabilities may be easily traced from the results, as will be shown. Values of other parameters in Table 1 are taken from the literature in accordance with the parameters already known [ν_1, ν_2: Hamilton (1971); ρ_1, ρ_2, k_2: Davis (1969); c_{g1}, c_{g2}: Simmons and Brace (1965); η, c_f: Kuchling (1971)].

Figure 6 shows how the excess pore pressure propagates in space and time. As expected, the pressure propagates faster for higher permeable sands. The time dependence

Table 1. Soil parameters of standard model

		z m	E dyne·cm^{-2}	ν	ρ %	k cm^2	c_g cm^2·dyne^{-1}
Sand layer	(1)	0– 32	2.0×10^9	0.47	45	15×10^{-9}	2.5×10^{-12}
Sandy clay layer	(2)	32–180	3.33×10^9	0.45	63	4×10^{-11}	2.0×10^{-12}

Pore fluid (water): $c_f = 5\cdot10^{-11}$ cm^2·dyne^{-1}, $\eta = 0.0165$ g·s^{-1}·cm^{-1} (20° C)

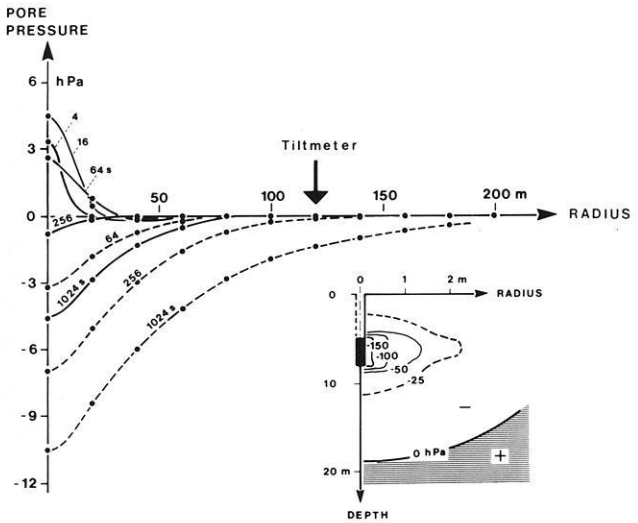

Fig. 6. Migration of pore pressure deficit after model calculations. Main diagram: change in pore pressure is plotted for depth 20 m, parameter is time in seconds from pump activation; solid and broken lines apply for permeabilities $15\cdot10^{-9}$cm^2 (standard model) and $15\cdot10^{-8}$cm^2 in sand layer. Inserted diagram: parameter is pore pressure change in hecto Pascals for standard model, time is 64 s from pump activation

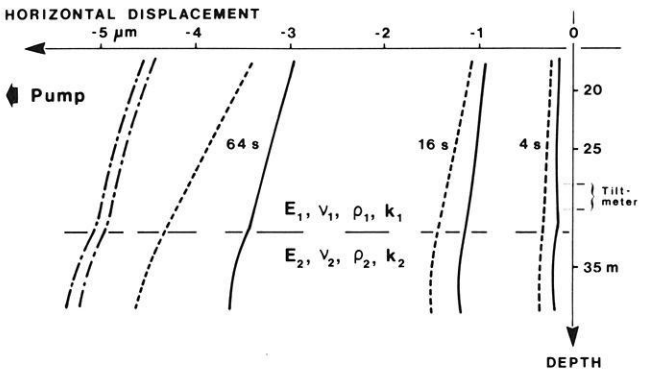

Fig. 7. Horizontal displacements for $r = 120$ m in the vicinity of the tiltmeter after model calculations. *Indexed lines:* parameter is time in seconds from pump activation, *solid lines* for standard model except $k_1 = 15\times10^{-8}$cm^2, *broken lines* for same model except $\nu_2 = 0.47$, i.e. no contrast in Poisson's ratio between two layers. *Hatched dotted lines:* radial decrease of displacements, *left curve* for $r = 120$ m, *right curve* for $r = 122$ m (standard model, 1,024 s from pump activation)

of the process can be normalized when k/η is replaced by the dimensionless quantity $k\cdot t/L$ where L is some characteristic length of the geometry of the experiment.

The initial increase of the pore pressure for $r < 30$ m requires some further remarks. Although plotted for the standard model only, the increase occurs equally if other parameters are chosen. The phenomenon has been found in many types of consolidation problems, both theoretically and experimentally (e.g. Cryer, 1963; Verruijt, 1969), and can be explained from the elastic behaviour of the aquifer. When the pore pressure decreases at the well screen, mobile water is attracted from the aquifer. The loss of water yields a decrease in soil volume. The contraction is seen as a negative load by the surroundings. Loading deformation propagates with seismic velocity, i.e. much faster than the deficit of the pore pressure diffuses. As a consequence, soil particles displace towards the negative load, inwardly generating a compression of the soil. Since the pore fluid opposes volume compression, the pore pressure increases in areas where it has not yet declined due to diffusion (see also inserted diagram in Fig. 6). Within the first 1,024 s, the standard model predicts the pore pressure at the location of the tiltmeter to vary within the range of the numerical noise, i.e. by less than 0.1 hPa. Applying a k_1-value 10 times higher already yields a pore pressure drop of 1.4 hPa after that time.

Clearly, significant soil displacements appear earlier at the tiltmeter location than any pressure drop. Radially horizontal displacements for some of the models calculated are plotted in Fig. 7. It is noticeable how the displacements are influenced by the contrast in Poisson's ratio of the two layers. As time progresses, the displacements increase more rapidly if there is no contrast. The depth of the layer intersection is of minor influence as long as the tiltmeter borehole is completely in the upper layer. Some 5–10 m below the intersection, the displacements decrease with depth, which is partly due to the clamped boundary at 180 m depth. The radial decrease of displacements shown in Fig. 7 corresponds to horizontal strains of -5×10^{-8}; respective vertical strains are positive and amount to 2×10^{-8}. Accordingly, the soil around the tiltmeter is found to be radially stretched; namely, more than twice as much as compressed vertically.

Referring to the observed tilt disturbances, the most essential results are summarized in Fig. 8. Herein the pump is simulated to run during a time span of 5 min. Tilt means the change in inclination of a vertical element, which – at the location of the tiltmeter – hardly differs from the change in inclination of a horizontal element. The tilt response following the shutdown of the pump is obtained by subtracting the inverse tilt response – shifted by 5 min – from the response for the persistently running pump (dotted lines). Computational results and observations are compatible within the shaded area. The vertical width of this area is estimated from uncertainties in both the amplitude of the pore pressure deficit at the well screen and the values of some soil parameters. Note that the observed tilt signal does not allow tilt variations shorter than 20 s to be resolved.

The initial 25-s section of curve A is identical to the

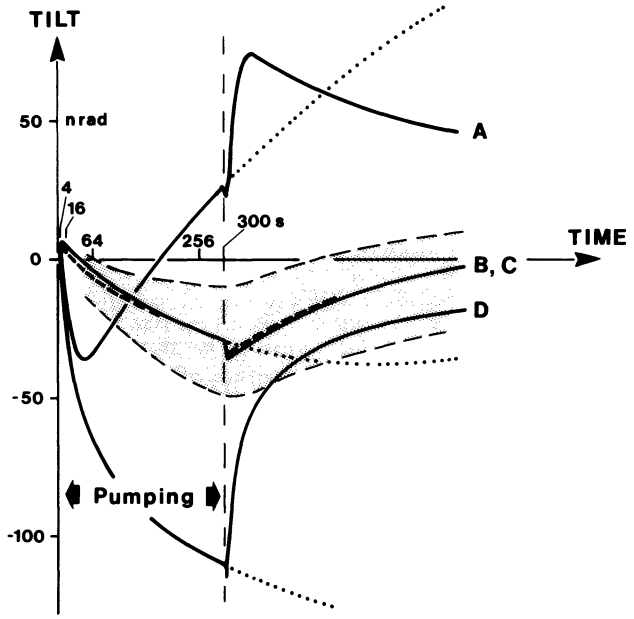

Fig. 8. Tilt response at location of tiltmeter due to pumping cycle lasting 5 min (linear time scale). A – standard model, except $k_1 = 15 \times 10^{-8}\text{cm}^2$; B – standard model (*solid line*); C – standard model, except $k_2 = 15 \times 10^{-9}\text{cm}^2$ (i.e. no permeability contrast between two layers, *broken line*); D – standard model, except $k_1 = 15 \times 10^{-8}$ cm^2 and $\nu_2 = 0.47$ (i.e. no contrast in Poisson's ratio between two layers); *shaded area:* consistent with observations

initial 300-s section of curve B except for a linear stretching of B due to a permeability 10 times lower. Curve D differs from A only in an absence of Poisson's ratio contrast between the two layers. Obviously, the deformation becomes sensitive to the parameter ν after some characteristic time, i.e. when the pore pressure starts to drop significantly at half the distance between the well and the tiltmeter borehole (Fig. 6). Neither curve A nor D fits the observations, nor do other models that are based on k_1 values as high as $15 \times 10^{-8}\text{cm}^2$. If the permeability of the aquifer was better than $5 \times 10^{-8}\text{cm}^2$, 5–10 times stronger tilt disturbances should have been recorded within the first minute after pump activation.

The tilt response of the standard model is consistent with the observations. This does not confirm the correctness of all the parameters applied. The permeability of the sandy clay layer, for example, is not constrained by any model within the first 300 s (see curve C). Other parameters, including the geometry of the standard model, may also vary considerably without destroying the compatibility condition. Still, the bulk in-situ permeability of the upper 30–40 m ranges among the parameters best constrained by the time variation of the tilt response.

So far, little has been said about the size of the region around the well that provokes the deformation at the location of the tiltmeter, i.e. the region to which we refer the permeability estimates. The source for the external deformation is the volume that decreases due to internal pore pressure drop. Naturally, if pumping continues, the size of this volume grows. Its shape is mainly determined by the shape of the well screen and variations in permeability around the well. Due to the diffusion process, the volume is not limited by a clearly defined boundary but can instead be described through concentric surfaces of equal pressure drop (see also Fig. 6) or, in other words, through isobars normalized to the hydrostatic pressure.

As for the size of the volume that is mostly efficient for the external deformation, there are two effects that oppose each other. Since the gradient of the pore pressure is a body force in Eq. (1), those parts of the volume that enclose the highest gradients seem to be mostly efficient. With cylindrical or spherical (but not plane strain) diffusion processes, the gradient of the diffusion variable increases towards the centre of the disturbance, regardless of how long the disturbance has already been active (Carslaw and Jaeger, 1959). This proves the innermost volume around the well screen to be mostly efficient for the external deformation.

An isobar of low percentage pressure drop is effective, however, in that it is both more expanded and closer to external points of deformation measurements than is a more central isobar of higher percentage pressure drop. Indeed, the computational results show that the effects due to the latter reasoning predominate those due to the former. The instantaneous deformation following the pump activation is provoked by the highest pressure gradient ever occurring around the well. Still, the deformation increases substantially when the volume of the pore pressure drop expands, thereby lowering the pressure gradient at the well screen.

Somewhat arbitrarily, we define the 5% pressure drop isobar as the one limiting the effective volume. Then, in our case, the standard model yields a radial penetration depth of 15 m after 5 min of pumping and a vertical penetration depth of 8 m.

Conclusions

There are two major implications from the findings, provided the approximations made are tenable.

First, bulk in-situ permeabilities of aquifers may be estimated from ground deformations that are caused by pumping. Since elastic deformation is provoked beyond the region of declined pore pressure, indications for the transmissivity of the soil are available up to distances where this deformation can be measured. The penetration depth of the method exceeds that of those methods that rely on well pressure fluctuations because it is controlled by the duration of the stimulated pore pressure disturbance. Most characteristic for the in-situ permeability is the time function of the deformation. Experiment expenses might be reduced to reasonable amounts if strong pressure signals are generated in the well so that less sensitive instruments fulfil the deformation measurements. A detailed description of tiltmeters and strainmeters used for geodynamic purposes has been given by Agnew (1985). Pumping could also be replaced by fluid injection, yielding a change in the sign of the soil displacements. In many cases it will be sufficient to install a tiltmeter or a strainmeter in a shallow borehole. Surface deformation due to temperature variation or wind stress can be separated from the deformation signal caused by pumping because the switch times of the pump are well known. Signal enhancement can be achieved when cyclic pulse tests are set up.

Second, the consolidation theory seems to be applicable to certain deformation phenomena observed with highly sensitive instruments (like earth tide meters). In particular, rainfall-induced water-table variations are believed to produce the most annoying noise in geodynamic signals (e.g.

Wood and King, 1977; Kümpel, 1982). Modelling these generally local phenomena improves the understanding of tilt and strain recordings that are obtained in tectonic regions for the purpose of earthquake prediction, for instance.

Acknowledgements. We owe our sincere thanks to Chris Beaumont, John Peters and Jochen Zschau for many fruitful discussions, to Michael Huszak who did laboratory experiments on soil samples and to Kathleen Helbig who made numerous helpful comments on the manuscript. Hans-J. Kümpel received a Killam postdoctoral fellowship at Dalhousie University in Halifax, Canada, where all the model calculations were done. The German Research Foundation (DFG) supported the tiltmeter experiment at Medelby. The comments of two unknown reviewers are gratefully acknowledged.

References

Agnew, D.C.: Strainmeters and tiltmeters. Reviews of Geophysics, submitted 1985

Biot, M.A.: General theory of three-dimensional consolidation. J. Appl. Phys. **12**, 155–164, 1941

Bodvarsson, G.: Confined fluids as strainmeters. J. Geophys. Res. **75**, 2711–2718, 1970

Booker, J.R., Small, J.C.: An investigation of the stability of numerical solutions of Biot's equations of consolidation. Int. J. Solids Structures **11**, 907–917, 1975

Bredehoeft, J.D.: Response of well-aquifer systems to earth tides. J. Geophys. Res. **72**, 3075–3087, 1967

Brown, R.H., Konoplyantsev, A.A., Ineson, J., Kovalevsky, V.S.: Groundwater studies. Studies and reports in hydrology, 7, Paris (UNESCO), 1972

Carslaw, H.S., Jaeger, J.C.: Conduction of heat in solids. Oxford: Clarendon Press 1959

Christian, J.T., Boehmer, J.W.: Plane strain consolidation by finite elements. J. Soil Mech. and Found. Div., ASCE **96**, 1435–1457, 1970

Cooper, H.H. Jr., Bredehoeft, J.D., Papadopulos, I.S., Bennett, R.R.: The response of well aquifer systems to seismic waves. J. Geophys. Res. **70**, 3915–3926, 1965

Cryer, C.W.: A comparison of the three-dimensional consolidation theories of Biot and Terzaghi. Q. J. Mech. Appl. Math. **16**, 401–412, 1963

Davis, S.N.: Porosity and permeability of natural materials. In: Flow through porous media, R.J.M. De Wiest, ed.: pp. 54–89, New York: Academic Press 1969

Davis, S.N., De Wiest, R.J.M.: Hydrogeology. New York: John Wiley and Sons 1966

Hamilton, E.L.: Elastic properties of marine sediments. J. Geophys. Res. **76**, 579–604, 1971

IMSL, Inc.: Twodepep, 5th ed. Houston: IMSL, Inc. 1983

Krauss, I.: Die Bestimmung der Transmissivität von Grundwasserleitern aus dem Einschwingverhalten des Brunnen-Grundwasserleitersystems. J. Geophys. **40**, 381–400, 1974

Kuchling, H.: Physik, Formeln und Gesetze. Köln: Buch- und Zeit-Verlagsgesellschaft mbH 1971

Kümpel, H.-J.: Neigungsmessungen zwischen Hydrologie und Ozeanographie. Ph.D. thesis, Univ. Kiel, 1982

Morland, L.W., Donaldson, E.C.: Correlation of porosity and permeability of reservoirs with well oscillations induced by earth tides. Geophys. J. R. Astron. Soc. **79**, 705–725, 1984

Nur, A., Byerlee, J.D.: An exact effective stress law for elastic deformation of rocks with fluids. J. Geophys. Res. **76**, 6414–6419, 1971

Ohkubo, T., Terasaki, A.: Physical property and seismic velocity of rock. OYO-Technical Note 22, translation from: Soil and Foundation **19**, 7, 1971 (in Japanese), 1977

Rhoads, G.H. Jr., Robinson, E.S.: Determination of aquifer parameters from well tides. J. Geophys. Res. **84**, 6071–6082, 1979

Robinson, E.S., Bell, R.I.: Tides in confined well-aquifer systems. J. Geophys. Res. **76**, 1857–1869, 1971

Simmons, G., Brace, W.F.: Comparison of static and dynamic measurements of compressibility of rocks. J. Geophys. Res. **70**, 391–398, 1965

Varga, P.: Investigation of earth tides by observing dilatational variations of the water table. Bull. d'Inform. Marrées Terrestres, P. Melchior (ed) **74**, 4319–4332, 1976

Verruijt, A.: Elastic storage of aquifers. In: Flow through porous media, R.J. M. De Wiest, ed.: pp 331–376, New York: Academic Press 1969

Wood, M.D., King, N.E.: Relation between earthquake, weather, and soil tilt. Science **197**, 154–156, 1977

Zschau, J.: Air pressure induced tilt in porous media. In: Proc. 8th Int. Symp. Earth Tides, Bonn 1977, M. Bonatz, P, Melchior eds.: pp. 418–433, Bonn: 1979

Received March 27, 1985; Revised version July 8, 1985
Accepted July 17, 1985